

Stability Analysis of Nonlinear Oscillations for AC-Fed Electric Arc Furnaces in Context of Bifurcation Dynamics

M. Varan¹, Y. Uyaroglu¹

¹*Department of Electrical and Electronics Engineering, Sakarya University, Esentepe Campus 54100-Sakarya, Turkey, phone: +902642955537
mvaran@sakarya.edu.tr*

Abstract—Bifurcation theory has been widely used to investigate dynamic behaviours of nonlinear components, and to make analytical answers on the formation of synchronous resonance, chaotic oscillations and ferroresonance oscillation phenomenon in electrical engineering. Bifurcation theory is also applied to perform stability analysis in nonlinear systems. This study aims to identify formations of nonlinear oscillations produced by AC-Fed Electric Arc Furnaces, in regard with bifurcation dynamics on the system. During the study, possible roles of small parameter changes of the sample arc furnace system around bifurcation points have been traced over time series analysis, phase plane analysis and bifurcation diagrams. A wide collection of useful dynamic analysis procedures for the exploration of studied arc furnace dynamics has been handled through the AUTO open-source algorithms.

Index Terms—AC-Fed electric arc furnace, AUTO open-source algorithms, bifurcation theory, nonlinear oscillations, stability analysis

I. INTRODUCTION

Nonlinear loads are the principal cause of power quality problems including voltage dips, harmonic distortion and flicker [1]. By this context, AC-fed electric arc furnace (EAF) should be categorized into an unbalanced, excessively nonlinear and time varying load. The nonlinear oscillations produced by EAF operation cause many difficulties to interconnected feed system. Harmonic and interharmonic injections to the feed system, unbalanced three phase voltages and currents due to the irregular nature of the electric arc, current randomness due to the rapid changes in lengths of electric arc and transient oscillations reasoned by the random movement of the melting material can be expressed into major ones of such these problems [2]. By its external effects on feed systems, EAF also accommodates very sensitive internal peculiarities. Any change from the system parameters results into significant changes in the behaviour of complete system dynamics. Such parameter changes sometimes may result into different degrees of complexity. The need for accurately understanding about

dynamical behaviours of smelting processes, several electric arc furnace models have been developed [3], [4]. Dynamic model representation should be encouraged also with nonlinear dynamic analysis methods. Among many nonlinear methods, bifurcation analysis method is chosen for investigating qualitatively the ways in which instabilities can take place in EAF.

Bifurcation theory has been widely used to investigate dynamic behaviours of nonlinear components, and to make analytical answers on formation of synchronous resonance, dynamical behaviour of induction machines, chaotic oscillations and Ferro resonance oscillations phenomenon in electrical engineering. Bifurcation theory is also one of the main techniques used to perform stability studies in nonlinear systems. This study aims for demonstrating relationships between formation of bifurcation dynamics and formations of nonlinear oscillations produced by EAF. The study specifically focuses effects of quasistatic changes in the feed system parameters on formation of nonlinear oscillations in EAF current and voltage. During the study, possible roles of small parameter changes of sample arc furnace system around bifurcation points have been traced over time series analysis, phase plane analysis and bifurcation diagrams.

This paper is organized as the follows. In Section 2, complicated dynamical behaviour of the nonlinear AC-fed electric arc furnace model is further investigated. In Section 3, extent of bifurcation theory is considered for stability analysis purposes. In Section 4, studied arc furnace model is analysed in context of bifurcation dynamics. A brief conclusion of study is presented in Section 5.

II. MODELLING OF AC-FED ELECTRIC ARC FURNACES

Electric arc furnaces (EAFs) are used in the production of aluminium, copper, lead, high-grade alloy steel, and other metals. EAFs are large, concentrated, dynamic, and time varying loads [5] and comprise a major portion of industrial loading on the bulk power system [6]. Electric arc furnaces are generally classified by their feed types. AC EAFs are fed by AC source which connected to furnace electrodes via a transformer, whereas DC EAFs connected to electrodes via DC rectifier. In this work AC EAF is considered as case study.

Manuscript received April 19, 2012; accepted October 21, 2012.

This work is supported in part by the Scientific Research Support Program Fund in Sakarya University with grant- number: 2011-50-02-008 (http://www.eee.sakarya.edu.tr/tr/arastirma_projeleri).

Based on the model presented in [2]–[4] an arc furnace can be represented by the following differential equation

$$K_1 r^n + K_2 r \frac{dr}{dt} = \frac{K_3}{r^{m+2}} i^2, \quad (1)$$

where r is the arc radius and resembles a state variable [7], m is the inner temperature effect (changes from 0 to 2 with integer steps; 0-large and colder arc length, 2-smaller and hotter arc length, 1-intermediate length and temperature) and n resembles non-dependence of the arc temperature from the arc radius, (changes from 0 to 2 with integer steps; 0 represents a non-dependence situation of the arc temperature on the arc radius) [2]. K_1 , K_2 , K_3 constants represent arc cooling effects. The parameters in (1) have a direct effect on the speed of convergence to the system stability, the arc V-I characteristics and on its equilibrium operation points. The effect of the internal furnace refractory is ignored in the model.

During the analysis process, $K_1=0.08$, $K_2=0.005$ and $K_3=3.0$ have been taken as fixed parameter for nominal operation points for arc furnace.

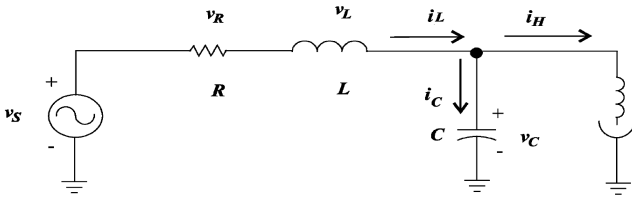


Fig. 1. Schematic diagram of the AC-Fed Arc furnace model.

Fig. 1 illustrates an AC-fed arc furnace connected to a power network [5]. Here, R and L represents the resistance and inductance of the power system, respectively, V_S shows magnitude of the AC feed, V_R and V_L holds the associated voltages, C is the capacitor bank connected parallel with the electric arc furnace, V_C is the voltage across the capacitor bank, L_H is the equivalent inductance [6] of the flexible connection cables, the electric arc furnace transformer and the electrodes [2].

After coupling modelled arc furnace to the network and appliance of Kirchhoff's current and voltage laws to the meshes and nodes of the circuit sketched in Fig. 1, following state equations can be written:

$$\begin{cases} \frac{di_L}{dt} = -\frac{R}{L} i_L - \frac{1}{L} v_C + \frac{1}{L} v_S, \\ \frac{dv_C}{dt} = \frac{1}{C} v_C - \frac{1}{C} i_H, \end{cases} \quad (2)$$

$$\begin{cases} \frac{di_H}{dt} = -\frac{1}{L_H} v_C - K_3 \frac{r^{-(m+2)}}{L_H} i_H, \\ \frac{dr}{dt} = K_3 \frac{r^{-(m+3)}}{K_2} i_H - K_1 \frac{r^{(n-2)}}{K_2} r, \end{cases} \quad (3)$$

where state variables of system are i_L – current magnitude of inductor, v_C –voltage magnitude across capacitor bank, i_H –

current magnitude flows into arc furnace electrodes, and r –radius of arc furnace [2], [3].

III. BIFURCATION THEORY

The knowledge of the bifurcation structure of a dynamical system is therefore important in order to understand the system's response to the changes in parameter values [7]. Bifurcation theory studies these qualitative changes in the phase portrait [8], [9]. Stability analysis of the system based on the bifurcation theory requires of a set of algebraic and/or differential equations which include state variables and parameters. In this study, dynamic model of the EAF is characterized by a set of parameter dependent differential equations [10], as follows

$$\dot{x} = f(x, \lambda), \quad (4)$$

where $x \in \mathfrak{R}^n$ represents vector of the dynamic state variables, and $\lambda \in \mathfrak{R}^k$ represents vector of system parameters that varies leisurely, transferring the state of system from one equilibrium point to another. In this paper K is restricted to be one, such that λ is a scalar value [8].

For the state equations of system given in (4), let's equilibrium point be $p_e = (x_e, \lambda)$, Hopf bifurcation appears when the following condition is satisfied:

- 1) The Jacobian matrix- JX has a simple pair of pure imaginary eigenvalues; i.e., $\gamma(\lambda_e) = \alpha(\lambda_e) \pm j\omega(\lambda_e)$ such that $\alpha(\lambda_e) = 0$ and $\omega(\lambda_e) > 0$, and no other eigenvalues with zero real parts.
- 2) $\frac{d\{\text{Re } \gamma(\lambda)\}}{d\lambda} \Big|_{\lambda = \lambda_e} = \frac{d\alpha(\lambda)}{d\lambda} \Big|_{\lambda = \lambda_e} \neq 0$. The Hopf

bifurcation is a catastrophe in which as one gradually changes the parameters in an ordinary differential equation, a fixed point suddenly changes to a limit cycle. Behaviours of oscillations define the type of Hopf. While small oscillations show that type of bifurcation is supercritical, growing oscillations show that type of bifurcation is subcritical [8], [9]. Stability of limit cycles and equilibrium points effect to each other and these behaviours also define overall system stability by regarding emerging of periodic orbits.

IV. BIFURCATION DYNAMICS OF STUDIED ARC FURNACE MODEL

This part of the study includes the representation of outputs for detailed bifurcation dynamics of studied arc furnace model. It is important to remark that system parameters are selected around industrial operation ranges [Appendix A]. Equilibrium point of the system is potentially depended on the change of the system parameters [2]. As sketched in Fig. 2 mentioned parameters represent a stable equilibrium point. This means that transient behaviour of the system finishes and system becomes a steady state in $t=48$ ms with $i=10.6298$.

With initial conditions, the system will be shown by

$$I_o = (i_{Lo}, v_{Co}, i_{Ho}, r_o, L), \quad (5)$$

where i_{L_o} – Inductor current of feed, v_{C_o} – Voltage across capacitor bank, i_{H_o} – Current flows into arc furnace electrodes, r_o – Arc furnace radius, L – Inductance of the power system.

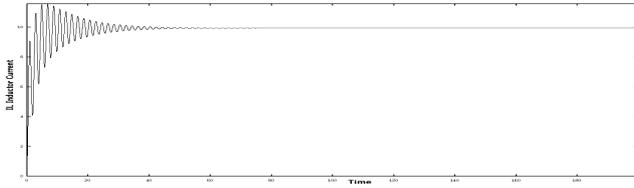


Fig. 2. After stabilization of AC-Fed Arc furnace inductor current.

Initial conditions parameters are taken $I_o = (10.6298, 0.315, 0.00134, 0.932177, 0.120)$. In this paper, bifurcation points are identified through combined assessments of eigenvalues. L is chosen as bifurcation parameter. In Fig. 3, bifurcation points are shown by PDB-1, PDB-3, PDB-5 and UHB-LP abbreviations.

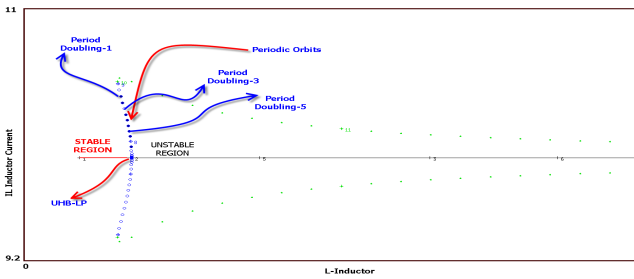


Fig. 3. Bifurcation diagram of AC-Fed Arc furnace.

As shown in Fig. 3, bifurcation diagram demonstrates change of i_L -inductor current in regard with change of inductance of feed. From PDB-1 to PDB-5 system oscillates around stability margins.

For PDB-1 point (i_L, v_C, i_H, r, L) is (9.24394, 0.66317, 11.40363, 5.44987, 0.6118734) and “first Lyapunov coefficient” is calculated as $-9.358964e+001$.

For PDB-3 point (i_L, v_C, i_H, r, L) is (9.3145056, 0.538464, 11.03236, 5.38086, 0.6120555) and “first Lyapunov coefficient” is found at $-1.964556e+001$.

For PDB-5 point (i_L, v_C, i_H, r, L) is (9.46237, 0.25699, 10.20492, 5.22250, 0.612729) and “first Lyapunov coefficient” is found at -5.964556 .

Unstable/supercritical Hopf bifurcation point is detected at $L=0.613548$. Real part of conjugate eigenvalues at UHB point is out of stability margins borders.

For UHB-LP point (i_L, v_C, i_H, r, L) is (9.57417, 0.04054, 9.57417, 5.09620, 0.613548) and “first Lyapunov coefficient” is $1.244568e-004$.

Fig. 4 depicts the changes of relevant eigenvalues of PDB-1, PDB-3, PDB-5 and UHB-LP at equilibrium points. The eigenvalues are calculated by substituting (PDB-1, PDB-3, PDB-5 and UHB-LP) values of the system equilibrium points into values of state variables in the Jacobian matrix. There are four eigenvalues for each equilibrium point because of system’s representation by four first order state equations.

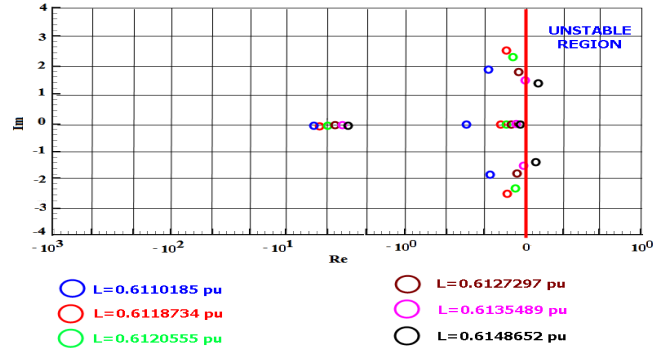


Fig. 4. Changes of eigenvalues at equilibrium point of system.

At the $L=0.6106534$ value, the eigenvalues are ($e_{1,2} = -0.172 \pm 2.02i$, $e_3 = -0.149$, $e_4 = -7.99$). It is clear that eigenvalues at that point are far from instability margin. At the $L=0.6118734$ (PDB-1) value, the eigenvalues are ($e_{1,2} = -0.153 \pm 2.56i$, $e_3 = -0.085$, $e_4 = -7.52$). At the $L=0.6120555$ (PDB-3) value, the eigenvalues are ($e_{1,2} = -0.148 \pm 2.22i$, $e_3 = -0.057$, $e_4 = -6.80$). At the $L=0.6127297$ (PDB-5) value, the eigenvalues are ($e_{1,2} = -0.082 \pm 1.93i$, $e_3 = -0.048$, $e_4 = -5.65$). It is clear that eigenvalues from PDB-1 to PDB-5 draw near stability margin border. At the $L=0.6135489$ (UHB-LP) value, the eigenvalues are ($e_{1,2} = 0.00004 \pm 1.37i$, $e_3 = -0.035$, $e_4 = -4.28$). For this point necessary condition for Hopf bifurcation is satisfied by the presence of complex conjugate eigenvalues with real part $\text{Re}[2] \cong 0$ and $\text{Re}[3] \cong 0$. Real part of conjugate eigenvalues at UHB point spills over into stability margins borders.

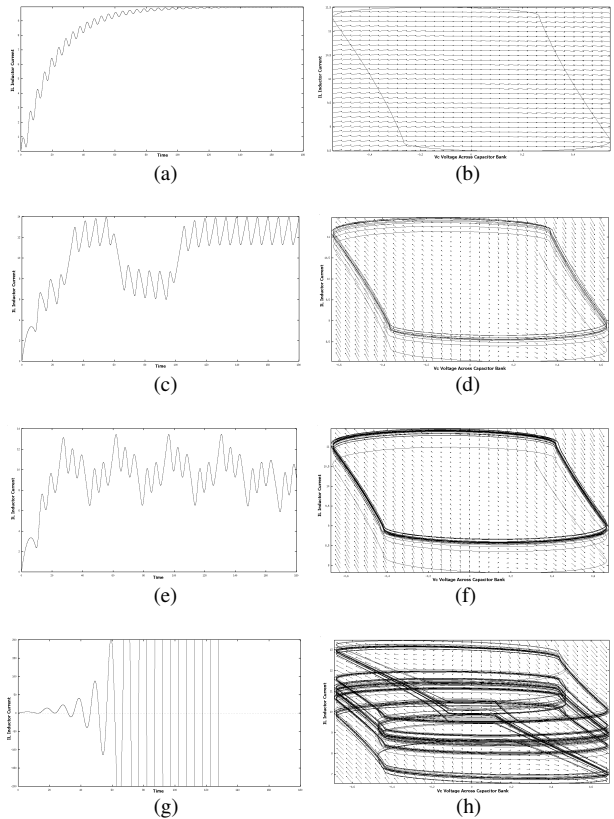


Fig. 5. Time series and phase portraits of period doubling branches.

UHB-LP has been detected at $L=0.613548$ value, after quasistatically perturbation near to this equilibrium point the

appearance of further bifurcations of periodic orbits (PDB-1, PDB-3 and PDB-5) are also detected and demonstrated in bifurcation diagram. Fig. 5 (a) shows time series and phase portraits at $L=0.6106534$ value. In Fig. 5 (c) and Fig. 5 (d), formation of PDB-1 is sketched via on time series of i_L -inductor current and i_L -inductor current and v_C -voltage across capacitor bank phase portraits at $L=0.6118734$ value, respectively. Fig. 5 (e) and Fig. 5 (f) shows formation of PDB-3 at $L= 0.6120555$ value. From PDB-1 to PDB-5, periodic oscillations of i_L -inductor current grow continuously. However, periodic oscillations fall into stability margins. Fig. 5 (g) and Fig. 5 (h) shows formation of UHB-LP at $L= 0.613548$ value.

Several cascade period-doubling bifurcations cause periodicity of the system solutions and finally create chaotic orbits on phase portraits. At UHB-LP point, periodic oscillations spill over into stability margins borders. The Lyapunov exponent at that point found to be 0.057, which confirms chaotic nature.

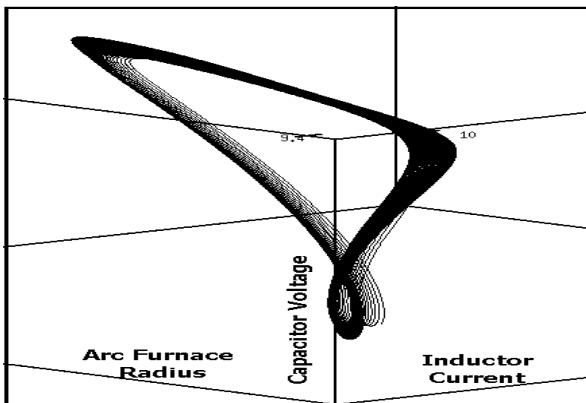


Fig. 6. Strange attractor formation near UHB-LP point.

Fig. 6 shows chaotic nature of arc furnace at UHB-LP point visually. As seen in Fig. 6 strange attractor formation satisfies -being unique in the motion of the system never repeats itself (non-periodic) - condition.

V. CONCLUSIONS

In this study, a stability analysis of nonlinear oscillations produced by AC-fed electric arc furnace in context of bifurcation dynamics has been presented. During study, possible roles of small parameter changes of sample arc furnace system around bifurcation points have been traced over time series analysis, phase plane analysis and bifurcation diagrams. It was observed that several cascade period-doubling bifurcations cause periodicity of the system solutions and finally create chaotic orbits on phase portraits. Unstable Hopf bifurcation and limit point were detected at $L= 0.613548$ value in which periodic oscillations spill over into stability margins borders. The Lyapunov exponent at that point was calculated as 0.057, which confirms chaotic nature. It should be remarked that the Hopf bifurcation was obtained for inductance values well within the system operation range.

APPENDIX A

TABLE I. SYSTEM PARAMETERS.

Parameters	Init. Cond.	Parameters	Init. Cond.
C	0.89	K_1	0.08
L	0.124	K_1	0.005
V_S	1	K_1	3
m	2	R	0.10
n	2	L_H	0.10

REFERENCES

- [1] L. Hocine, D. Yacinea, B. Kamela, K. M. Samiraa, "Improvement of Electrical Arc Furnace Operation with An Appropriate Model", *Energy*, vol. 34, no. 9, pp. 1207–1214, 2009. [Online]. Available: <http://dx.doi.org/10.1016/j.energy.2009.03.003>
- [2] A. Medina, M. A. Gómez-Martínez, C. R. Fuerte-Esquivel, "Application of Bifurcations Theory to Assess Nonlinear Oscillations Produced by AC Electric Arc Furnaces", *IEEE Trans. on Power Delivery*, vol. 20, no. 2, pp. 801–807, 2005. [Online]. Available: <http://dx.doi.org/10.1109/TPWRD.2005.844289>
- [3] E. Acha, A. Semlyn, N. Rajakovick, "A harmonic domain computational package for nonlinear problems and its applications to electric arcs", *IEEE Trans. on Power Delivery*, vol. 5, pp. 1390–1397, 1990. [Online]. Available: <http://dx.doi.org/10.1109/61.57981>
- [4] H. Samet, M. E. H. Golshan, "Employing stochastic models for prediction of arc furnace reactive power to improve compensator performance", *IET Gen. Transmission and Distribution*, vol. 2, no. 1, pp. 505–515, 2008. [Online]. Available: <http://dx.doi.org/10.1049/iet-gtd:20070320>
- [5] E. O'Neill – Carrillo, et al., "EMTP implementation and analysis of nonlinear load models", *Electric Power Components and Systems*, vol. 29, no. 9, pp. 809–820, 2001.
- [6] A. Yazdani, Mariesa L. Crow, J. Guo, "An Improved Nonlinear STATCOM Control for Electric Arc Furnace Voltage Flicker Mitigation", *IEEE Trans. on Power Delivery*, vol. 24, no. 4, pp. 2284–2290, 2009. [Online]. Available: <http://dx.doi.org/10.1109/TPWRD.2009.2027508>
- [7] E. Bagarinao, T. Nomura, S. Sato, "Time Series-Based Bifurcation Analysis", *Mathematical Analysis of Random Phenomena on Science and Engineering - Theories and Applications*, pp. 14–23, 1999.
- [8] J. D. Crawford, "Introduction to bifurcation theory", *Reviews of Modern Physics*, vol. 63, no. 4, pp. 991–992, 1991. [Online]. Available: <http://dx.doi.org/10.1103/RevModPhys.63.991>
- [9] H. S. Strogatz, *Nonlinear Dynamics and Chaos*. Cambridge-Perseus publishing, 2000.
- [10] R. Garcia-Kasusky, D. Torres-Lucio, C. Fuerte-Esquivel, "Assessment of the SVC's Effect on Nonlinear Instabilities and Voltage Collapse in Electric Power Systems", in *Proc. of the 2003 IEEE Power Engineering Society General Meeting*, Toronto Canada, 2003. [Online]. Available: <http://dx.doi.org/10.1109/PES.2003.1271067>